*Inorg. Chem.* **2008**, *47*, 11807−11815

# A Continuous Symmetry Measure of $[4Fe-4S]^{+}$ Core Distortions and Analysis of Supramolecular Synthons in Crystal Structures of $(Et_4N)_3[Fe_4S_4Cl_4]\cdot Et_4NCl$ at 100 and 295 K

**Karl S. Hagen* and Mohammad Uddin**

*Department of Chemistry, Emory University, Atlanta, Georgia 30322*

Received August 11, 2008

Distortions of the $[4Fe-4S]^{+}$ cores of synthetic models from $T_d$ symmetry are analyzed in terms of the continuous symmetry measures (CSM, $S(T_d)$), and these are related to lattice effects in terms of the supramolecular synthon terminology common to crystal engineering of small molecule structures. The small tetragonal compression to $D_{2d}$ from idealized $T_d$ symmetry observed at low temperature is attributed to environmental factors. New members of the isomorphous series of compositional variations of double salts of the air-sensitive reduced cluster $(Et_4N)_3[Fe_4S_4Cl_4]\cdot Et_4NCl$ (**1**) are prepared in modest yield by treatment of $FeCl_2$ with NaHS, or $(Et_4N)_2[FeCl_4]$ with $Et_4NSH$ and a base. The crystals are isomorphous with the corresponding $HS^{-}$ ligated cluster. Crystal data: tetragonal, $P\bar{4}2_1c$, $Z = 2$, $a = b = 12.2550$ (4), $c = 16.278$ (1) Å at 100 K, and $a = b = 12.385$ (1), $c = 16.344$ (2) Å at 295 K. The crystallographically imposed $S_4$ symmetry obtained with sterically unincumbering ligands affords a better view of the intrinsic geometry of the core structure. The cocrystallization of the halide ion affords the opportunity to compare three types of weak C−H···X hydrogen bonds, or hydrogen bridges, between tetraalkylammonium cations and anions within the same crystal lattice. The C···$Cl^{-}$ distances (3.590 and 3.634 at 100 K increase to 3.616 and 3.655 Å, respectively, at 295 K) are virtually temperature independent, indicative of hard hydrogen bridges, whereas the C···Cl−Fe distances are 3.702−3.718 Å at 100 K but are 3.753−3.764 Å at room temperature, suggesting a softer hydrogen bridge. A similar trend applies to the two sets of C···$\mu_3$-S distances (3.766−3.788 Å and 3.594−3.604 Å at 100 K and 3.821−3.848 Å and 3.614−3.676 Å at room temperature). The longer hydrogen bridges are more linear (170°) than the shorter ones (134°). The core distortions are correlated with spatial distribution of cations around the clusters.

## Introduction

Protein crystallography has played a crucial role in defining the structure of native iron−sulfur clusters but, until recently, at a generally much lower resolution than is available with synthetic models.[1] The low confidence level in core dimensions of early protein structures was dispelled by accurate high-resolution structures of synthetic models,[2] which have typically displayed tetragonal distortions of the [4Fe−4S] heterocubane clusters from idealized $T_d$ symmetry.[3] The distortions are not consistent over all structures, however, and the role of lattice effects in the crystals have been evoked to account for variations in structure.[4,5] The "softness"[6] or "plasticity"[7] of the reduced core structures in particular has been recognized and is particularly evident with the crystal structure determinations of high symmetry ($T_d$ point group) cores in both oxidized[8] and reduced[9] clusters. Within the past decade, advances in protein science and crystallography have made it possible to obtain high-resolution crystal

* To whom correspondence should be addressed. E-mail: khagen@emory.edu.

(1) Stout, C. D. Metal Ions in Biology. In *Iron−Sulfur Proteins*; Spiro, T. G. Ed.; Wiley Interscience, New York, 1982; Vol. *4*, Ch. 3.
(2) Herskovitz, T.; Averill, B. A.; Holm, R. H.; Ibers, J. A.; Phillips, W. D.; Weiher, J. F. *Proc. Natl. Acad. Sci. USA* **1972**, *69*, 2437–2441.
(3) Rao, P. V.; Holm, R. H. *Chem. Rev.* **2004**, *104*, 527–559.
(4) Mascharak, P. K.; Hagen, K. S.; Spence, J. T.; Holm, R. H. *Inorg. Chim. Acta* **1983**, *80*, 157–170.
(5) Kanatzidis, M. G.; Baenziger, N. C.; Coucouvanis, D.; Simopoulos, A.; Kostikas, A. *J. Am. Chem. Soc.* **1984**, *106*, 4500–4511.
(6) Carney, M. J.; Papaefthymiou, G. C.; Spartalian, K.; Frankel, R. B.; Holm, R. H. *J. Am. Chem. Soc.* **1988**, *110*, 6084–6095.
(7) Czernuszewicz, R. S.; Macor, K. A.; Johnson, M. K.; Gewirth, A.; Spiro, T. G. *J. Am. Chem. Soc.* **1987**, *109*, 7178–7187.
(8) Williams, J. B.; Köckerling, M. *Chem. Commun* **2001**, 1380–1381.
(9) Segal, B. M.; Hoveyda, H. R.; Holm, R. H. *Inorg. Chem.* **1998**, *37*, 3440–3443.

10.1021/ic801533q CCC: $40.75 
Published on Web 11/12/2008

structures[10−12] that are on a par with those of model clusters, permitting detailed comparison of weak interactions between the cluster and its immediate environment. The protein environment of $[4Fe-4S]^{n+}$ ($n = 0, 1, 2, 3$) clusters greatly influence structure and redox potential[13,14] and, as a result, their most common function as electron transfer agents.[15] These developments call for a new approach in the analysis of these structures first in terms of the distortions of the [4Fe−4S] cores and, second, in the intermolecular forces and how these might effect the core structures. Two significant developments in the analysis of structures now makes this possible. The first is the continuous symmetry measure (CSM) of Avnir and co-workers[16,17] and the second is the field of crystal engineering of small molecules.

CSM is a quantitative measure $S(G)$ of the deviations of a structure of $N$ vertexes whose coordinate vectors $\{Q_k, k = 1, 2, ..., N\}$ deviate from a specific perfect symmetry group $G$ (having coordinate vectors $\{P_k, k = 1, 2, ..., N\}$, and is given by the following equation,

$$S(G) = \min \frac{\sum_{k=1}^{N} |Q_k - P_k|^2}{\sum_{k=1}^{N} |Q_k - Q_o|^2} \times 100$$

where $Q_o$ is the coordinate vector of the structure's center of mass.[18] It has been used to analyze the relationships of several inorganic structures to classic polyhedra, and we apply it as an effective numerical way to compare distortions from the idealized $T_d$ symmetry in [4Fe−4S] clusters.[19] The typical tetragonal distortions that have been observed in the [4Fe−4S] cores are evident by a set of four near-parallel Fe−S bond lengths that distinguish themselves by either being shorter than (a tetragonal compression) or longer than (a tetragonal elongation) the other eight Fe−S bonds. The continuous symmetry measure affords the $S_4$ nature of the three mutually perpendicular $S_4$ axes of the cubane cores, so the relative degree of distortion becomes more evident. The CSM approach has been used to describe distortion pathways between different shapes,[20] including the eight-vertex polyhedra that include [4Fe−4S] clusters.[21] The field of crystal engineering is, in part, the study and application of supramolecular synthons, or the forces that hold the components of a crystal together.[22] Its methodologies have been widely applied in the field of solid state chemistry of molecular systems but less so in the description of crystal structures of synthetic models in bioinorganic chemistry.[23] As with the symmetry maps identified by the CSM method, the efforts leading to the methodologies of crystal engineering are a result of mining the extensive database of high-resolution crystal structures provided by the Cambridge Crystallographic Data Center.[24]

One category of recently appreciated synthons is D−H···A (donor/acceptor) hydrogen bonds, in which the donors are C−H bonds rather than the more conventional D−H···A (D/A = F, N, O, or Cl). Desiraju[25] advocates use of the term "hydrogen bridge bonds" in this situation, as the intention is to distinguish traditional hydrogen bonds from these weaker, but still essential, supramolecular synthons. C−H···A hydrogen bridge bonds are the primary intermolecular interactions in crystals of neutral organic molecules[26,27] and organometallic compounds.[28] Even more robust are the charge-assisted hydrogen bridge bonds (CAHB) of the type $R_3N^+C-H\cdots S$ found in crystals of clusters having the general formula $(R_4E)_m[Fe_nS_nX_4]$ (where E = N, R is alkyl or E = P, R is aryl; $m = 0-4$; $n = 2, 4$; and X is an anionic ligand), as well as in other charged coordination complexes.

The purpose of this report is to apply the above analyses on the products of a simple one-pot synthesis and crystallization of members of the isomorphous series of compositional variations of double salts having the general formula $(Et_4N)_3[Fe_4S_4X_4]\cdot Et_4NY$ (X = Y = Cl (**1**); X = SH, Y = Cl (**2**); and X = Cl, Y = Cl/SH (**3**)). The analysis of the supramolecular synthons in these crystals feature three related CAHB in the same lattice: $R_3N^+-C-H\cdots X^-$, $R_3N^+-C-H\cdots X-Fe$, and $R_3N^+-C-H\cdots\mu_3$-$SFe_3$. This emphasis on the intermolecular forces in solid state structures will be helpful not only in describing high-resolution protein structures, but will also facilitate the design of functional solid state models of iron sulfur proteins that are capable of mimicking their electron transfer function and, perhaps more importantly, their role in catalysis.

## Experimental Section

**Preparation of Compounds.** All manipulations were carried out in a dry dinitrogen-filled glovebox using anhydrous solvents that


(10) Parisini, E.; Capozzi, F.; Lubini, P.; Lamzin, V.; Luchinat, C.; Sheldrick, G. M. *Acta Crystallogr.* **1999**, *D55*, 1773–1784.
(11) Dauter, Z.; Wilson, K. S.; Sieker, L. C.; Meyer, J.; Moulis, J. M. *Biochemistry* **1997**, *36*, 16065–16073.
(12) Liu, L.; Nogi, T.; Kobayashi, M.; Nozawa, T.; Miki, K. *Acta Crystallogr.* **2002**, *D58*, 1085–1091.
(13) Holm, R. H.; Kennepohl, P.; Solomon, E. I. *Chem. Rev.* **1996**, *96*, 2239–2314.
(14) Flint, D. H.; Allen, R. M. *Chem. Rev.* **1996**, *96*, 2315–2334.
(15) Dey, A.; Francis, E. J.; Adams, M. W. W.; Babini, E.; Takahashi, Y.; Fukuyama, K.; Hodgson, K. O.; Hedman, B.; Solomon, E. I. *Science* **2007**, *318*, 1464–1468.
(16) Zabrodsky, H.; Peleg, S.; Avnir, D. *J. Am. Chem. Soc.* **1992**, *114*, 7843–7851.
(17) Zabrodsky, H.; Peleg, S.; Avnir, D. *J. Am. Chem. Soc.* **1993**, *115*, 8278–8289.
(18) (a) Pinsky, M.; Avnir, D. *Inorg. Chem.* **1998**, *37*, 5575–5582. (b) Alvarez, S.; Avnir, D.; Llunell, M.; Pinsky, M. *New J. Chem.* **2002**, *22*, 996–1009.
(19) Because the structures are initially normalized, only the symmetry, not the size, of structures are compared by CSM. The size is reflected in the independently calculated polyhedral volumes.
(20) Casanova, D.; Cirera, J.; Llunell, M.; Alemany, P.; Avnir, D.; Alvarez, S. *J. Am. Chem. Soc.* **2004**, *126*, 1755–1763.
(21) Casanova, D.; Llunell, M.; Alemany, P.; Alvarez, S. *Chem.—Eur. J.* **2005**, *11*, 1479–1494.
(22) Desiraju, G. R. *Angew. Chem., Int. Ed. Engl.* **1995**, *34*, 2311–2327.
(23) (a) Holm, R. H.; Ibers, J. A.; In *Iron−Sulfur Proteins*; W. Lovenberg, W. Ed.; Acadamic Press, New York, 1977; Ch. 7. (b) Ibers, J. A.; Holm, R. H. *Science* **1980**, *209*, 223–235.
(24) Allen, F. H.; Kennard, O. *Chem. Des. Automat. News* **1993**, *8*, 31–37.
(25) Desiraju, G. R. *Acc. Chem. Res.* **2002**, *5*, 565–573.
(26) Taylor, R.; Kennard, O. *J. Am. Chem. Soc.* **1982**, *104*, 5063–5070.
(27) Steiner, T.; Desiraju, G. R. *Chem. Commun.* **1998**, 891–892.
(28) Braga, D.; Grepioni, F. *Acc. Chem. Res.* **2000**, *33*, 601–608.

were used as received after sparging with dinitrogen. The complex $(Et_4N)_2[FeCl_4]$ was prepared as reported,[29] and $FeCl_2$ and $Et_4NSH$ were used as obtained from Cerac.

**$(Et_4N)_3[Fe_4S_4Cl_4]\cdot(Et_4N)Cl$. (1). Method 1.** Combining nearly colorless DMF solutions of 0.20 g of $Et_4NHS$ (1.2 mmol in 25 mL) and 0.12 g of triethylamine (1.2 mmol) with 0.55 g $(Et_4N)_2[FeCl_4]$ (1.2 mmol in 25 mL) formed an intensely colored, almost black, solution. The solution was stirred for 20 min and was left undisturbed at room temperature for one week. Crystals of the complex $(Et_4N)_3[Fe_4S_4Cl_4]\cdot Et_4NCl$ (0.052 g, 16%) were physically separated from a fine, insoluble, amorphous black powder.

**Method 2.** An acetonitrile solution of 0.28 g of $(Et_4N)_2[FeCl_4]$ (0.61 mmol), 0.07 g of $FeCl_2$ (0.55 mmol), and 0.15 g of NaOPh (1.3 mmol in 40 mL) was stirred for 10 min, and then the off-white solution was filtered to remove NaCl. The filtrate was treated with 0.20 g of $Et_4NSH$ (1.25 mmol) dissolved in 10 mL of acetonitrile. The color of the solution turned to black, then 40 mL of diethyl ether was added and the solution was kept at room temperature. After four days, black crystals formed along with some black powder (0.21 g). The crystals were isolated and recrystallized by cooling an acetonitrile solution. After 24 h, crystals of the complex $(Et_4N)_3[Fe_4S_4Cl_4]\cdot Et_4NCl$ (0.030 g, 10%) formed and were collected.

**$(Et_4N)_3[Fe_4S_4(SH)_4]\cdot(Et_4N)Cl$. (2).** Crystals by method 1 above, except that 320 mg of $Et_4NSH$ (2.0 mmol) was added to 228 mg of $(Et_4N)_2[FeCl_4]$ (0.50 mmol). The sample was recrystallized by cooling a warm DMF solution to −20 °C.

**X-ray Structure Determinations.** Crystals were collected on filter paper in the glovebox and immediately immersed in Paratone oil to protect them from oxidation and/or solvent loss. They were removed from the glovebox to a microscope stage for sample selection and mounting in or on Rayon loops and then transferred to the diffractometer where they were bathed in a dinitrogen stream from an Oxford Instruments Cryostream Series 700 low temperature device. Data were collected on a Bruker D8 SMART Apex CCD diffractometer using standard procedures (see CIF files in the Supporting Information). The structures were solved and refined using standard procedures, and hydrogen atoms on the cations were included in calculated positions and are not corrected. The largest peak in the difference map of **2** was chosen as the H atom on the SH group. As there are no hydrogen bond acceptors, the H atom is probably disordered over positions that do not interfere with the C−H···S interaction.

The CSM calculations are part of the Platon crystallographic package of programs invoked with the CALC NONSYM command.[30] The cif files were edited to contain only that fragment of the structure under consideration: the $Fe_4S_4$ unit or $Fe_4S_4X_4$ (X = Cl, or S of SH or SR). Shape parameters and polyhedral volumes were obtained using CrystalMaker (David Palmer, www.CrystalMaker.com).

**Other Physical Measurements.** $^1$H NMR spectra were recorded on a General Electric QE-PLUS 300 MHz, a Varian Inova 400, or a General Electric Omega-600 spectrometer in $CD_3CN$, $CD_3COCD_3$, or $CDCl_3$ and referenced to tetramethylsilane. Electronic absorption spectra were collected on a Shimadzu UV-3101PC, UV−vis−NIR scanning spectrophotometer.

## Results and Discussion

**Synthesis and Characterization. Results.** Iron(II) halides or complexes, such as $(Et_4N)_2[FeCl_4]$ and $(Et_4N)_2[Fe_2(OPh)_2X_4]$ (X = Cl, Br)[31,32] using a 1:1 ratio of iron halide to phenoxide (eq 1), react with $Et_4NHS$ or NaHS in acetonitrile or dimethylformamide solutions to form intensely colored solutions that deposit some black amorphous solid along with crystalline isomorphous double salts: $(Et_4N)_3[Fe_4S_4X_4]\cdot Et_4NY$ for X = Y = $Cl^-$ (**1**) and X = $HS^-$, Y = Cl (**2**) (eqs 2−4). We find that better yields are obtained in the coordinating solvent, DMF, than in acetonitrile, in which a greater amount of insoluble black powder forms. We have not yet been successful in isolating bromo-ligated clusters by this method.

$$2FeX_2 + 2NaOPh + 2Et_4NX \rightarrow (Et_4N)_2[Fe_2(\mu\text{-}OPh)_2X_4] + 2NaX \quad (X = Cl, Br) \quad (1)$$

$$2(Et_4N)_2[Fe_2(\mu\text{-}OPh)_2Cl_4] + 4Et_4NSH \rightarrow (Et_4N)_3[Fe_4S_4Cl_4] + 4PhOH + 4Et_4NCl \quad (2)$$

$$4(Et_4N)_2[FeCl_4] + 8Et_4NSH \rightarrow (Et_4N)_3[Fe_4S_4Cl_4] + 4H_2S + 12Et_4NCl \quad (3)$$

$$4(Et_4N)_2[FeCl_4] + 12NaSH \rightarrow (Et_4N)_3[Fe_4S_4(SH)_4] + 4H_2S + 12NaCl + 4Et_4NCl \quad (4)$$

Crystal growth is a supramolecular process involving recognition by solvated species of surface sites on the growing crystal. This process may not discriminate between chloride and hydrosulfide; components of the potential equilibria in eq 5 and crystalline samples composed of the mixture: $(Et_4N)_3[Fe_4S_4Cl_{4-n}(SH)_n]\cdot Et_4NCl_{1-m}(SH)_m$ ($n$ = 0−4, $m$ = 0−1) could form;

$$[Fe_4S_4Cl_4]^{3-} + 4HS^- \rightleftharpoons [Fe_4S_4Cl_{4-n}(SH)_n]^{3-} + nCl^- + (4-n)HS^- \quad (5)$$

Purity was determined by electrospray ionization mass spectroscopy (ESI-MS), where the difference in natural abundance of isotopes of Cl and S affords distinct spectral patterns that can be used to differentiate between separate species in $[Fe_4S_4Cl_{4-n}(SH)_n]^{x+}$ ($n$ = 0−4, see Supporting Information Figure S-1).

**Discussion.** Of the five potential oxidation states of the iron−sulfur clusters with cores $[Fe_4S_4]^{n+}$ ($n$ = 0−4), all but the $n$ = 4 cluster have previously been isolated by appropriate choice of terminal ligand on iron. The original "as-isolated" form, using common reagents and due care to prevent air oxidation or hydrolysis, contain the $[Fe_4S_4]^{+2}$ core. The single electron reduced cluster $[Fe_4S_4]^{+1}$ is considerably more susceptible to oxidation by adventitious chemical oxidants during preparation, purification, and characterization. Thus, models of this oxidation state were initially isolated by chemical reduction of the prepurified clusters $(R_4N)_2[Fe_4S_4(SR)_4]$ using strong chemical reductants; although this

(29) Gill, N. G.; Taylor, F. B.; Hatfield, W. E.; Parker, W. E.; Fountain, C. S.; Bunger, F. L. *Inorg. Synth.* **1968**, 9.
(30) As implemented in PLATON; Spek, A. L. *J. Appl. Crystallogr.* **2003**, *36*, 7–13.
(31) Coucouvanis, D.; Greiwe, K.; Salifoglou, A.; Challen, P.; Simopoulos, A.; Kostikas, A. *Inorg. Chem.* **1988**, *27*, 593–594.
(32) Emori, S.; Nakashima, M.; Mori, W. *Bull. Chem. Soc. Jpn.* **2000**, *73*, 81–84.

**Table 1.** X-ray Crystallographic Data for $(Et_4N)_3[Fe_4S_4X_4]\cdot Et_4NY$ (X = Y = Cl (**1**); X = SH, Y = Cl (**2a**); X = Cl, Y = Cl/SH (**3**))

| crystal data for | **1b** | **1a-LT** | **1a-RT** | **1c** | **3** | **1d** | **2a** |
|---|---|---|---|---|---|---|---|
| formula | $4(C_8H_{20}N)\cdot Cl_4Fe_4S_4\cdot Cl$ | | | | | | $4(C_8H_{20}N)H_4Fe_4S_8Cl$ |
| F000 | 1106 | | | | | | 1106 |
| Mr | 1049.89 | | | | | | 1040.36 |
| $D_{calcd.}$ (g cm$^{-3}$) | 1.431 | 1.426 | 1.391 | 1.422 | 1.376 | 1.396 | 1.384 |
| $T$ (K) | 100 (2) | 100 (2) | 295 (2) | 100 (2) | 298 (2) | 295 (2) | 295 (2) |
| crystal system space group, $Z$ | Tetragonal, $P\bar{4}2_1c$, 2 | | | | | | |
| X-ray radiation, $\lambda$ | Mo K$\alpha$, 0.71073 Å | | | | | | |
| $\mu$, (mm$^{-1}$) | 1.64 | 1.63 | 1.59 | 1.63 | 1.58 | 1.6 | 1.55 |
| $a$ = (Å) | 12.2465 (5) | 12.2550 (4) | 12.385 (1) | 12.2784 (3) | 12.435 (1) | 12.3771 (8) | 12.4153 (4) |
| $c$ = (Å) | 16.241 (1) | 16.278 (1) | 16.334 (2) | 16.2649 (9) | 16.385 (3) | 16.309 (2) | 16.198 (1) |
| $V$ = (Å$^3$) | 2435.8 (2) | 2444.7 (2) | 2507.0 (4) | 2452.1 (2) | 2533.7 (5) | 2498.4 (4) | 2496.8 (2) |
| color | black | | | | | | |
| crystal size (mm$^3$) | 0.28 × 0.22 × 0.17 | 0.32 × 0.24 × 0.11 | | 0.29 × 0.10 × 0.07 | 0.37 × 0.17 × 0.13 | 0.31 × 0.13 × 0.11 | 0.18 × 0.16 × 0.15 |
| $\theta$ (°) | 2.5−27.5 | 2.1−33 | 2.1−26.0 | 2.1−30.0 | 2.3−31.8 | 2.1−26.5 | 2.3−30 |
| indep., $I > 2s(I)$ refl. | 2803, 2768 | 4457, 4241 | 2466, 2145 | 3571, 3112 | 2914, 2724 | 2590, 2420 | 2454, 2312 |
| R[$F^2 > 2\sigma(F^2)$] | 0.023 | 0.034 | 0.031 | 0.043 | 0.034 | 0.042 | 0.054 |
| $w$R($F^2$), S | 0.060, 1.2 | 0.087, 1.15 | 0.074, 0.96 | 0.086, 0.96 | 0.072, 1.04 | 0.101, 1.16 | 0.100, 1.04 |

approach was successful only for aryl thiolates and not for the more reducing alkyl thiolates. A "one-pot" synthesis was developed for the latter, using reactions of iron(II) precursors such as $(Et_4N)_2[Fe_4(SEt)_{10}]$ with $(Et_4N)SH$.[33] More recently, the reaction of $[Fe(PEt_3)_2Cl_2]$ with $(Et_4N)SH$ and $Na_2S$ directly affords the simplest structural model of reduced ferredoxins: $[Fe_4S_4(SH)_4]^{3-}$.[9]

**Crystal Structures.** The crystal structure of this double salt is isomorphous to the previously reported structure of $(Et_4N)_3[Fe_4S_4(SH)_4]\cdot(Et_4N)Cl$.[9] As described in Table 1, seven sets of data were collected on six crystals: two exclusively at low temperature (100 K, **1b** and **1c**), three at ambient temperature (**1d**, **2**, and **3**), and one at both (**1a-LT** and **1a-RT**). All diffraction data were consistent with primitive tetragonal unit cells and the space group $P\bar{4}2_1c$. The variations in cell dimensions are suggestive of the presence of members of the series $(Et_4N)_3[Fe_4S_4Cl_{4-n}(SH)_n]\cdot Et_4NCl_{1-m}(SH)_m$ ($n$ = 0−4, $m$ = 0−1) but, alone, are not sufficient to distinguish between them.

We chose this series in spite of the inherent difficulty of using X-ray diffraction to differentiate the isoelectric $Cl^-$ and $SH^-$ by analysis of electron density maps because, as has been shown for $[Fe_4S_4X_4]^{2-}$ (X = Cl, SH),[23] the difference in Fe−X bond lengths can be used to distinguish them. However, even here ambiguity remains as the mixture of Cl and SH at one site will exhibit an average bond length with unexceptional thermal parameters, so a single crystal structure determination may not be sufficient to establish the limiting distances for Fe−Cl and Fe−SH. This limitation has previously been demonstrated by Yoon and Parkin[34] with a series of Zn−X (X = Me, Cl, I) structures and has also been seen in $[Fe_2S_2X_4]^{2-}$ (X = Cl, Br).[35]

$[4Fe-4S]^{n+}$ clusters are usually described as "cubane-type" structures.[3] When such a structure contains two interpenetrating tetrahedra of identical size and composition it has $O_h$ symmetry; when the tetrahedra are of identical size but have different composition, it has $T_d$ symmetry. By extension, when $Fe_4$ and $S_4$ tetrahedra are no longer the same size, the six faces of the cube become nonplanar rhombs, and the twelve triangles form an irregular dodecahedron, also called a triakis tetrahedron with $T_d$ symmetry. Our analysis uses Pilati and Forni's molecular symmetry determination (MOLSYM) program[36] and the continuous symmetry measure (CSM, S($G$)—a measure of the deviation of a structure from symmetry group $G$) of Zabrodsky and co-workers.[16,17] The $[4Fe-4S]^+$ core of **2a** (S($T_d$) = 0.01) and **2b**[9] (S($T_d$) = 0.00) exhibits near perfect $T_d$ symmetry. Somewhat greater distortions are seen in **1a-LT**, where the terminal $HS^-$ have been replaced by more electronegative $Cl^-$ (S($T_d$) = 0.01). This is the familiar tetragonal distortion toward $D_{2d}$ in which deviations are greater for two of the three mutually perpendicular $S_4$ axes (S($S_4$) = 0.01) than the third (S($S_4$) = 0.00, see Table 2 and Supporting Information). As compiled in Table 2, greater tetragonal distortions from $T_d$ symmetry of the core of **1** are evident at low temperature (S($T_d$) = 0.04 at 100 K) than at room temperature.

To emphasize the spacial arrangement of CAHB in the crystal, the $[Fe_4S_4X_4]^{n-}$ clusters are completely described as triakis tetrahedra, made of electronegative $S_4^*$ and $X_4$ tetrahedra. The supramolecular synthons between these tetrahedra, the anions $Cl^-$ or $SH^-$, and the cationic $^+N(CH_2)_4$ tetrahedra (see Figures 1 and 2) are the "glue" that maintains the isomorphous crystal structures of $(Et_4N)_3[Fe_4S_4Cl_{4-n}(SH)_n]\cdot Et_4NCl_{1-m}(SH)_m$ ($n$ = 0−4, $m$ = 0−1). They consist of parallel stacks of anions located on alternating crystallographic $S_4$ sites (Wyckoff positions $a$ and $b$) along the $c$-axes and center of a tetragonal cell. A single cation in the asymmetric unit sits on a general position such that each anion is surrounded by four cations (Figure 1).

The nonconventional hydrogen bridge bonds between them are summarized in Table 3 and are highlighted in color in Figure 2. Those CAHB involving the monatomic Y consist of four short contacts—H(7b)···Y, 2.64−2.71 Å; C(7)···Y, 3.582−3.617 Å; C(7)−H−Y, 160−161°—and two longer ones—H···Y, 2.83−2.89 Å; C(1)···Y, 3.629−3.671 Å;

(33) Hagen, K. S.; Watson, A. D.; Holm, R. H. *Inorg. Chem.* **1984**, *23*, 2984–2990.
(34) Yoon, K.; Parkin, G. *J. Am. Chem. Soc.* **1991**, *113*, 8414–8418.
(35) Tonon, C.; Ierno, H.; Laugier, J.; Greneche, J.-M.; Jordanov, J. *Chem. Ber.* **1997**, *130*, 235.
(36) (a) Pilati, T.; Forni, A. *J. Appl. Crystallogr.* **1998**, *31*, 503–504. (b) Pilati, T.; Forni, A. *J. Appl. Crystallogr.* **2000**, *33*, 417.

**Table 2.** CSM[30] for distortions from $T_d$ symmetry for $(Et_4N)_3[Fe_4S_4X_4]\cdot Et_4NY$ and Other Clusters Where Organic Groups Were Excluded for Calculations of $[Fe_4S_4X_4]^{3-}$ Clusters and $[Fe_4S_3]^+$ Cores[a]

| | $[Fe_4S_4]^+$ | | | | | | | | | $CgN_x$ | | | |
|---|---|---|---|---|---|---|---|---|---|---|---|---|---|
| | | $S(S_4)$ | | | Fe−S (Å) | | | | | | Cg···N | | |
| | $S(T_d)$ | $x$ | $y$ | $z$ | ∥ | ⊥ | ⊥ | Fe−X | X···C | S*···C | $x^b$ | ob | lel | ref, CSD refcode |
| $(Et_4N)_4[Fe_4S_4(SH)_4]Cl$ **2b** | 0.000 | 0.000 | 0.000 | 0.000 | 2.309 | 2.310 | 2.309 | 2.317 | 3.798 | 3.860 | 8 | 6.49 | 6.61 | 9, NUSRIC |
| $(Et_4N)_4[Fe_4S_4(SH)_4]Cl$ **2** | 0.010 | 0.008 | 0.008 | 0.000 | 2.300 | 2.313 | 2.314 | 2.326 | 3.760 | 3.833 | 8 | 6.46 | 6.59 | this work |
| $(Et_4N)_4[Fe_4S_4Cl_4]Cl$ **1a-RT** | 0.014 | 0.010 | 0.011 | 0.001 | 2.305 | 2.322 | 2.322 | 2.288 | 3.754 | 3.830 | 8 | 6.46 | 6.62 | this work |
| $(Et_4N)_4[Fe_4S_4Cl_4]Cl$ **1a-LT** | 0.045 | 0.034 | 0.034 | 0.000 | 2.294 | 2.325 | 2.320 | 2.293 | 3.710 | 3.766 | 8 | 6.42 | 6.57 | this work |
| $(Et_4N)_4[Fe_4S_4Cl_4]Cl$ **1b-LT** | 0.037 | 0.028 | 0.028 | 0.001 | 2.291 | 2.316 | 2.321 | 2.289 | 3.702 | 3.768 | 8 | 6.40 | 6.56 | this work |
| $(Et_4N)_4[Fe_4S_4Cl_4]Cl$ **1c-LT** | 0.040 | 0.030 | 0.030 | 0.000 | 2.292 | 2.314 | 2.319 | 2.287 | 3.718 | 3.788 | 8 | 6.42 | 6.57 | this work |
| $(Et_4N)_4[Fe_4S_4Cl_4]Cl$ **1d-RT** | 0.010 | 0.007 | 0.008 | 0.000 | 2.304 | 2.317 | 2.310 | 2.282 | 3.753 | 3.821 | 8 | 6.46 | 6.62 | this work |
| $(Et_4N)_4[Fe_4S_4X]Y$ **3-RT** | 0.011 | 0.008 | 0.008 | 0.000 | 2.314 | 2.323 | 2.328 | 2.294 | 3.765 | 3.676, 3.846 | 8 | 6.48 | 6.65 | this work |
| $(Me_4N)_3[Fe_4S_4(SEt)_4]$ | 0.075 | 0.054 | 0.058 | 0.004 | 2.293 | 2.320 | 2.327 | 2.315 | 3.840 | 3.48−3.57 | 2 + 4 | 6.44 | 5.64 | 33, COZXUK |
| $(Et_4N)_3[Fe_4S_4(S^tBu)_4]\cdot MeCN$ | 0.136 | 0.056 | 0.046 | 0.128 | 2.297 | 2.319 | 2.338 | 2.300 | 3.57−3.77 | 3.63−3.68 | 3 + 1 | 5.73, 6.66 | 6.01, 6.02 | 33, COZXOE |
| $(Et_4N)_3[Fe_4S_4(SBzl)_4]$ | 0.086 | 0.028 | 0.058 | 0.078 | | | | | | | 4 | 5.73 5.81 | | 37, BZTFEA |
| $(Et_4N)_3[Fe_4S_4(SBzl)_4]\cdot DMF$ | 0.099 | 0.023 | 0.088 | 0.062 | | | | | | | 3 + 2 | 5.81−6.01 | 6.53−6.65 | 38, RAPSEG |
| $(Et_3MeN)_3$ $[Fe_4S_4(SPh)_4]$ | 0.184, 0.103 | 0.106, 0.022 | 0.022, 0.025 | 0.163, 0.085 | | | | | | | 4 + 2 | 5.66−5.94 | 6.38−6.57 | 40, PSFEEA |
| $(Et_4N)_3[Fe_4S_4(S\text{-}p\text{-}C_6H_4Br)_4]$ | 0.150 | 0.040 | 0.148 | 0.090 | | | | | | | 4 + 2 | 5.72−5.92 | 6.39 | 39, BUTFAX |
| $(Me_4N)_3[Fe_4S_4(SPh)_4]\cdot 2MeCN$ | 0.332 | 0.172 | 0.274 | 0.084 | 2.340 | 2.270 | 2.300 | 2.300 | 3.82−3.99 | 3.560 | 4 + 2 | 5.57−5.71 | 6.57 | 45, GAPXEA |
| $(Me_4N)_3[Fe_4Se_4(SPh)_4]\cdot 2MeCN$ | 0.706 | 0.169 | 0.355 | 0.684 | 2.490 | 2.38,2.42 | 2.410 | | 3.72−3.92 | 3.620 | 4 + 2 | 5.78−5.81 | 6.51 | 45, GAPXIE |
| $(Et_4N)_3[Fe_4S_4(OPh)_4]$ | 0.513 | 0.109 | 0.195 | 0.510 | 2.300 | 2.320 | 2.340 | 1.920 | 3.25−3.48 | 3.66, 3.83 | 4 + 2 | 5.64− 5.79 | 6.34 | 41 |
| $(Bu_4N)_3[Fe_4S_4(CN)_4]$ | 0.021 | 0.021 | 0.018 | 0.017 | | | | 2.023 | | | 6 | 5.94 | | 40, JAHXEW |
| $(Et_4N)_3[Fe_4S_4(S\text{-}o\text{-}C_6H_4S^tBu)_4]$ | 0.295 | 0.178 | 0.260 | 0.034 | | | | | | | 3 + 2 | 5.87−6.04 | 6.53−6.88 | 47, VAMJOI |
| $(Et_4N)_3[Fe_4Se_4(SPh)_4]$ | 2.060 | 0.420 | 0.970 | 2.009 | 2.488 | 2.39−2.43 | | | | | 4 | 5.89−6.19 | | 46, SUVWUB |

[a] Metrical distances in Å. [b] $x$ = number of near neighbor cation nitrogens. When $x = m + n$, $m$ N with Cg···N < 6.3Å and $n$ N with 6.3 Å < Cg···N < 7 Å.

C(1)−H−Y, 137−139°—that, collectively, make up the two tetrahedra of an irregular $(R_3N^+C-H(1b))_4\cdots Cl\cdots(H(7b)-CN^+R_3)_4$ dodecahedron. The shorter contacts are oblique to the $S_4$ axis ($\beta$(H(7b)) = 77.6°), but the longer ones are more closely aligned with it ($\beta$(H(1b)) = 27.2°). Although we observe no spread in these distances when determined under low temperature conditions, the structure obtained from room temperature data shows less than 0.5% lengthening of these contacts. The corresponding distances for crystal **3** are slightly longer, possibly because in this crystal Y is a mixture of $HS^-$ and $Cl^-$.

All of the CAHB distances between the cations and $[Fe_4S_4X_4]^{3-}$ cluster are longer than those between the cations and the isolated chloride ions. In addition, a greater increase in the C−H···$\mu_3$−S−$Fe_3$ and C−H···Cl−Fe distances, 2 and 4%, respectively, is observed upon warming to room temperature. This suggests that these interactions are "softer" than those to $Cl^-$ and that interactions to the core sulfides are more robust than the significant, although weaker, interionic ones between cation and terminal ligands. Core sulfides exhibit a stronger interaction with the $R_3N^+CH_2Me$ methylenes—H···($\mu_3$-S), 2.84−2.93 Å; C···($\mu_3$-S), 3.594−3.676 Å; C(7)−H−($\mu_3$-S), 133−135°—than with the methyls: H···($\mu_3$-S), 2.80−2.90 Å; C···($\mu_3$-S), 3.766−3.848 Å; C−H−($\mu_3$-S), 170−172°). The high end of the ranges above correlate with the softer SH terminal ligands. These weak interactions with the terminal ligands (H···X, 2.77−3.00 Å; C···X, 3.702−3.798 Å; C−H−X, 157−159°) are not as definitive a means of distinguishing between Cl and SH as are the Fe−X distances that range from 2.289 to 2.326(1) Å in the structures reported here (see Table 3). On the basis of our analysis and comparison of the Fe−X distances in the oxidized clusters, we attribute the 2.289 Å bond to terminal Fe−Cl and the 2.326 (1) Å bond to Fe−SH (which is slightly longer than that found in **2b**).[9]

The lack of organic ligands on the clusters described here isolates the intermolecular interactions to CAHB ($R_3^+NC-H\cdots S/Cl$), as opposed to the more complex combination of intermolecular interactions with clusters having bulky or complex organic ligands (as in X = SEt, StBu, SBzl, SPh, S−$C_6H_4$−*p*-Br, or OPh). Invariably, when organic ligands are present the $[Fe_4S_4(X)_4]^{3-}$ clusters exhibit greater distortions from $T_d$ symmetry (X = SH, S($T_d$), 0.02−0.11; Cl, 0.23−0.61; SEt, 1.67;[33] $SCH_2Ph$, 1.35;[37,38] S′Bu, 3.19;[33] and OPh, 3.96) than do the $[4Fe-4S]^+$ cores (S($T_d$) 0.00 for SH to 0.51 for S′Bu, Table 2). When the alkyl thiolates are replaced by aromatic thiolates in $(Et_4N)_3[Fe_4S_4(SC_6H_4-p-Br)_4]$,[39] S($T_d$) is 1.95 and 0.15 for cluster and core, respectively. There are two clusters in the asymmetric unit of $(Et_3MeN)_3[Fe_4S_4(SPh)_4]$[40] and S($T_d$) is 0.184 for one but only 0.10 for the other, and the clusters do not show $T_d$


(37) Berg, J. M.; Hodgson, K. O.; Holm, R. H. *J. Am. Chem. Soc.* **1979**, *101*, 4586–4593.

(38) Gloux, J.; Gloux, P.; Laugier, J. *J. Am. Chem. Soc.* **1996**, *118*, 11644–11653.

(39) Stephan, D. W.; Papaefthymiou, G. C.; Frankel, R. B.; Holm, R. H. *Inorg. Chem.* **1983**, *22*, 1550–1557.

(40) Laskowski, E. J.; Frankel, R. B.; Gillum, W. O.; Papaefthymiou, G. C.; Renaud, J.; Ibers, J. A.; Holm, R. H. *J. Am. Chem. Soc.* **1978**, *100*, 5322–5337.

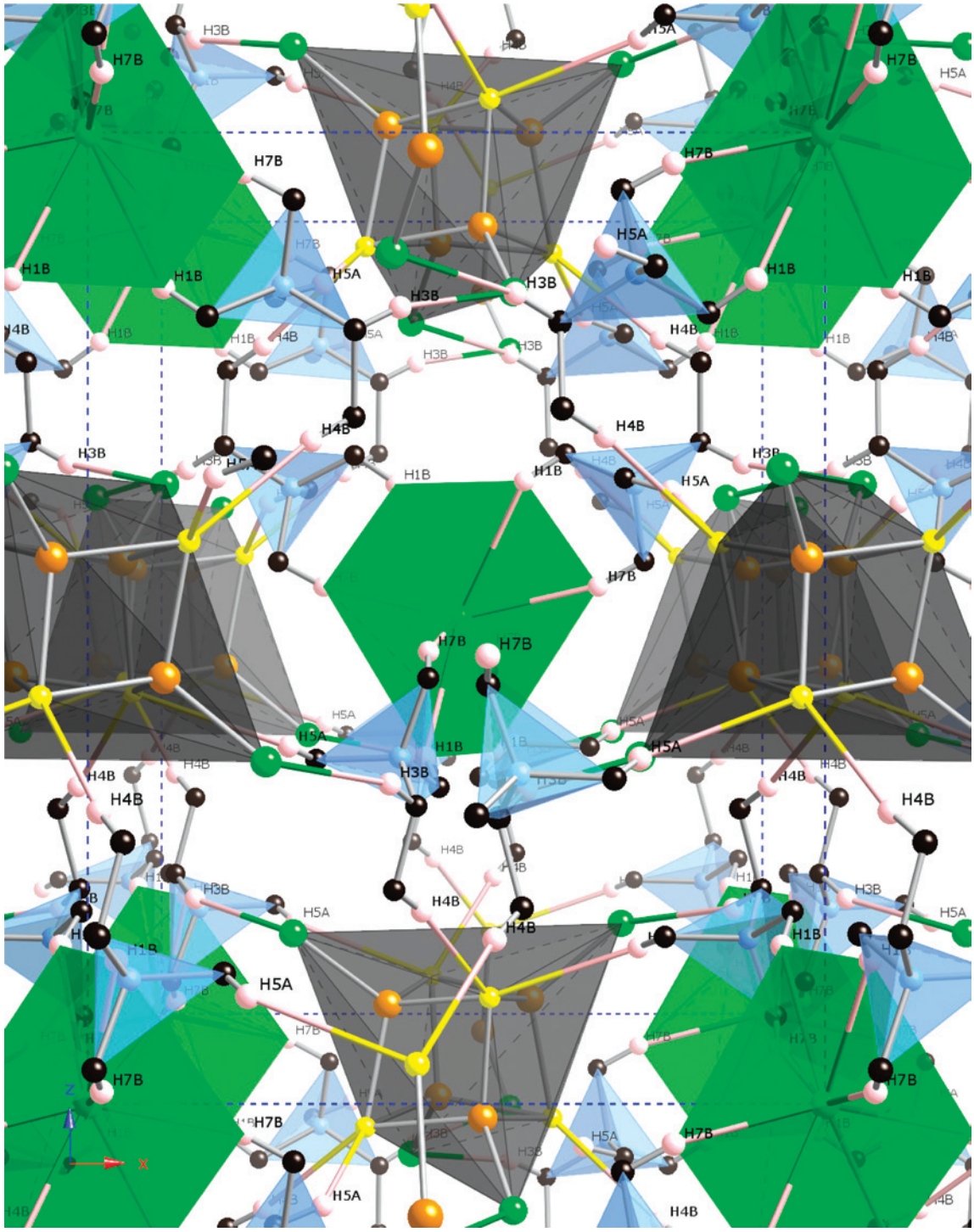


**Figure 1.** Packing diagram of $(Et_4N)_3[Fe_4S_4Cl_4]\cdot(Et_4N)Cl$ at room temperature viewed approximately down the *a* axis. $Fe_4S_4Cl_4$ clusters as gray, $Cl^-\cdots(HC)_8$ are green irregular dodecahedra, and N are blue tetrahedra, with $CH_3$ groups and C−H hydrogens not involved in C−H···X interactions omitted for clarity.

symmetry although the latter does show approximate $D_{2d}$ point group ($S(D_{2d})$, 0.556). The distortions are even more dramatic with the phenoxide cluster, $(Et_4N)_3[Fe_4S_4(OPh)_4]$,[41] where $S(T_d)$ is 3.96 for the cluster and 0.51 for the core, and phenoxides incorporate stronger C−H···O interactions in addition to the C−H···$\mu_3$-S bridge bond. The smaller spread in CSM for $[4Fe-4S]^+$ cores than that of $[Fe_4S_4X_4]^{3-}$ fragments of the clusters suggests that the cores have an intrinsic high symmetry and that distortions are caused by the supramolecular synthons of the crystal.

The structure to show this effect most dramatically is that of $(Bu_4N)_3[Fe_4S_4(CN)_4]$, which resides on a crystallographic $C_3$ axis in space group $R3c$.[42] The $[4Fe-4S]^+$ core has $S(T_d) = 0.021$, whereas inclusion of cyanide C affords $S(T_d) = S(T_{23}) = 0.834$ for the $[Fe_4S_4C_4]$ cluster, and the complete

(41) Hagen, K. S. unpublished results.

(42) Scott, T. A.; Zhou, H.-C. *Angew. Chem. Intl. Ed.* **2004**, *43*, 5628–5631.

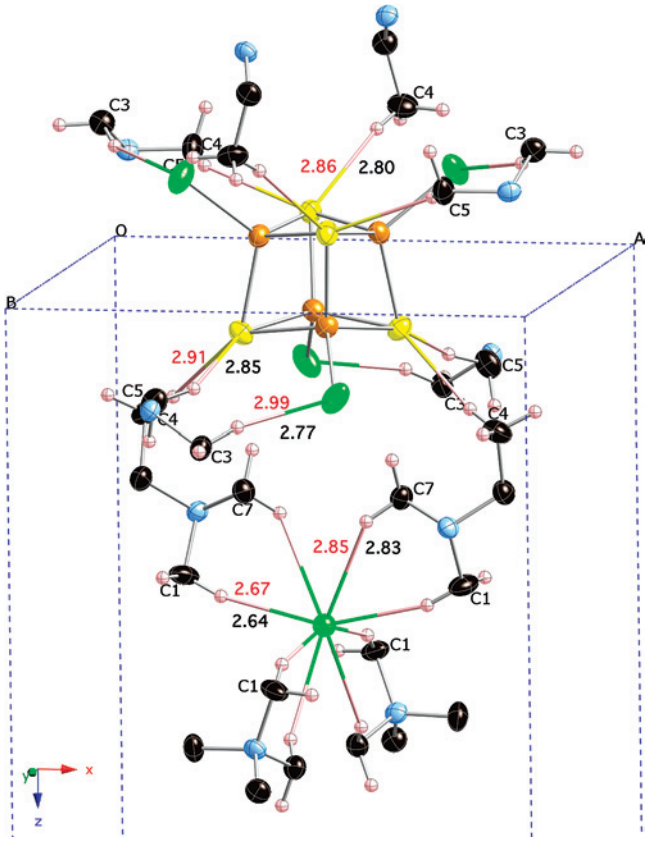


**Figure 2.** Thermal ellipsoid plot (50% probability level for data collected at 100 K) of $(Et_4N)_3[Fe_4(\mu_3\text{-}S)_4Cl_4]\cdot(Et_4N)Cl$, the $Cl^-$ (on $S_4$ axes = *c* axis and center of *ab* face) and those portions of the $Et_4N^+$ involved in C−H···X interactions with these anions. Fe in brown, S in yellow, Cl in green, N in blue, C−H···X bonds in color, and lengths (Å) given in black (100 K) and red (295 K).

$[Fe_4S_4(CN)_4]^{3-}$ cluster is not recognized as being close to $T_d$ symmetry ($S(T_{23}) = 2.86$) because of the significant bend in three of the four Fe−CN groups. The tilt in these $CN^-$ ligands are the result of a $R_3N^+C-H\cdots N'C$ $\pi$ hydrogen bond (C(1)···H, 2.90 Å; N(1)···H(36), 2.81 Å; C(1)−H−C(3), 142°; N(1)−H−C(3), 165°). The other cyanide nitrogen is equidistant to six hydrogens at 3.25 Å. Thus, the crystallography supports the $3Fe^{(II)}$ and $1Fe^{(III)}$ formal oxidation states of the cluster from both the intracluster dimensions and the intermolecular interactions. The tetragonal distortions from $T_d$ symmetry are much more pronounced and less variable in the more oxidized $[4Fe-4S]^{2+}$ cores. These generally appear as tetragonal compressions, although exceptions include a core elongation in $(Me_3NCH_2CONH_2)_2[Fe_4S_4(S^tBu)_4]$[43] and the crystallographically imposed $T_d$ symmetry of $(K(18C6))_4[FeCl_4][Fe_4S_4Cl_4]$, where the cluster is surrounded by a regular array of $K^+$.[44]

**Distribution of Cations around Cluster.** The $[Fe_4S_4X_4]^{3-}$ clusters are surrounded by eight cations whose nitrogens form the vertices of a dodecahedron, the center of which ($C_g$) is the center of each $Fe_4$ tetrahedron (Figure 3). Four of these nitrogens, $N_{lel}$ form a tedrahedron elongated along the crystallographic $S_4$ axis ($C_g\cdots N_{lel}$, 6.56−6.62 Å) and the other four, $N_{ob}$, form a tetrahedron that is flattened relative to this axis ($C_g\cdots N_{ob}$, 6.40−6.49 Å). An octahedron of chloride ions, each surrounded by a tetrahedron of cations, form bridges to neighboring clusters. The cations bridge the clusters such that the $N_{lel}$ adjacent to one cluster occupy the $N_{ob}$ positions about adjacent clusters. The symmetric disposition of cations around the cations is reflected in the high symmetry of the $[Fe_4S_4]^+$ cores reported here. A discernible trend relates the shorter Fe−S bonds parallel to the columns of cation interspersed anions. This situation also occurs in the $(Me_4N)_3[Fe_4S_4(SEt)_4]$ structure,[33] which also contains columns of clusters separated by cations along a crystallographic $S_4$ axis. In this case, the structure consists of a network of vertex-sharing octahedra of six cations surrounding each cluster. Both the octahedra and clusters exhibit tetragonal compressions along the $S_4$ axis (four Fe−S, 2.29 Å; two $C_g\cdots N_{lel}$, 5.64 Å; eight Fe−S, 2.32 Å; and four $C_g\cdots N_{ob}$, 6.44 Å). The $(Et_4N)_3[Fe_4S_4(S^tBu)_4]\cdot MeCN$ structure[33] consists of chains of clusters in distorted squares of cations that share two vertices along a diagonal that also coincides with the tetragonal compression of the cluster (four Fe−S, 2.297 Å; two $C_g\cdots N_{lel}$, 6.01 Å; eight Fe−S, 2.30−2.338 Å; and two $C_g\cdots N_{ob}$, 5.73 and 6.65 Å). The $(Me_4N)_3[Fe_4S_4(SPh)_4]\cdot 2MeCN$ structure[45] also contains the same chains of clusters in more regular squares of cations that share two vertices along a square diagonal that coincides with a crystallographically imposed 2-fold axis. The most notable feature is a tetragonal elongation of the cluster perpendicular to the $CgN_4$ squares (two Fe−S, 2.27 Å; parallel to two $C_g\cdots N$ at 5.57 and 5.63 Å; two Fe−S, 2.30 Å; parallel to two $C_g\cdots N$ at 5.71; and the two longer Fe−S bonds at 2.34 Å that are parallel to the S−C bonds of the ligands). Similar structures and distortions are seen for $[Fe_4Se_4(SPh)_4]^{3-}$ clusters (Table 2).[45,46] Other less-symmetric cores are associated with bulky ligands and correspondingly less-symmetric arrangements of cations.[47]

**Relationship of Models to Proteins.** There are eight conventional hydrogen bonds involving inorganic sulfide and thiolate sulfur in low potential ferredoxins. Only two such bonds, limited to the cysteinate sulfurs, are found in a more hydrophobic pocket in high-potential iron proteins (HiPIP). These clusters are surrounded by hydrophobic residues, resulting in protein/cluster interactions of the much weaker C−H···S hydrogen bridge type bonds discussed below. The CAHB interactions delineated above are comparable to those of protein-encapsulated $[4Fe-4S]^{2+/3+}$ clusters in hydrophobic pockets in the HiPIP and are not as evident in the $[4Fe-4S]^{2+}$ cores of low potential Ferredoxin (Fd) that are found in hydrophilic pockets rich in N−H···S hydrogen bonds. All but one of the sulfurs in the Fd (PDB:2FDN) have N−H···S hydrogen bonds to amides, including all but one of the inorganic sulfides of the [4Fe−4S] clusters. However, there are only two such bonds to the HiPIP cluster

(43) Walters, M. A.; Roche, C. L.; Rheingold, A. L.; Kassel, S. W. *Inorg. Chem.* **2005**, *44*, 3777–3779.
(44) Willems, J. B.; Köckerling, M. *Chem. Commun.* **2001**, 1380–1381.
(45) Carney, M. J.; Papaefthymiou, G. C.; Whitener, M. A.; Spartalian, K.; Frankel, R. B.; Holm, R. H. *Inorg. Chem.* **1988**, *27*, 346–352.
(46) Hauptman, R.; Schneider, J.; Chen, C. *Henkel Acta Cryst, C55* **1999**, 194–196.
(47) Carney, M. J.; Papaefthymiou, G. C.; Frankel, R. B.; Holm, R. H. *Inorg. Chem.* **1989**, *28*, 1497–1503.

**Table 3.** Selected Bond Lengths, Angles, and Shape Parameters for $(Et_4N)_3[Fe_4S_4X_4]\cdot Et_4NY$

| | **1aLT** | **1b** | **1c** | **1a-RT** | **1d** | **3** | **2a** | **2b**, ref 23 |
|---|---|---|---|---|---|---|---|---|
| *T*, K | 100 | 100 | 100 | 295 | 295 | 295 | 297 | 213 |
| Fe−S ∥[a] | 2.2944(6) | 2.2906(5) | 2.2918(9) | 2.305(1) | 2.304(1) | 2.3138(9) | 2.300(1) | 2.309(1) |
| Fe−S ⊥[a] | 2.3253(6) | 2.3163(5) | 2.3137(9) | 2.322(1) | 2.317(1) | 2.3226(8) | 2.313(1) | 2.310(1) |
| Fe−S ⊥[a] | 2.3202(6) | 2.3210(5) | 2.3193(9) | 2.3219(9) | 2.310(1) | 2.3283(8) | 2.314(1) | 2.309(1) |
| Fe-X | 2.2926(6) | 2.2886(5) | 2.2870(9) | 2.288(1) | 2.282(1) | 2.2935(8) | 2.326(1) | 2.317(2) |
| Fe···Fe | 2.7809(5) | 2.7761(5) | 2.7721(8) | 2.7862(9) | 2.782(1) | 2.7965(7) | 2.7584(9) | 2.764(1) |
| Fe···Fe | 2.7843(5) | 2.7778(5) | 2.7762(8) | 2.7908(9) | 2.786(1) | 2.7999(7) | 2.761(1) | 2.764(1) |
| compression: Fe···Fe (%)[b] | 0.12 | 0.06 | 0.15 | 0.16 | 0.14 | 0.12 | 0.09 | 0 |
| Fe−S (%)[b] | 1.2 | 1.2 | 1.1 | 0.7 | 0.4 | 0.5 | 0.6 | 0 |
| *r*, *β*, (*z*-Fe); Vol (Å$^3$)[c] | 1.704, 54.7, 2.54 | 1.701, 54.7, 2.52 | 1.699, 54.6, 2.52 | 1.708, 54.6, 2.56 | 1.705, 54.65,2.54 | 1.714, 54.76,2.58 | 1.690, 54.7, 2.48 | 1.692, 54.76,2.49 |
| *r*, *β*, (*z*-S*); Vol (Å$^3$) | 2.232, 55.7, 5.71 | 2.229, 55.5, 5.71 | 2.228, 55.4, 5.67 | 2.230, 55.1, 5.69 | 2.227, 55.1,5.67 | 2.238, 55.1,5.75 | 2.235, 55.1, 5.73 | 2.233, 54.70,5.71 |
| *r*, *β*, (*z*-X); Vol (Å$^3$) | 3.995, 52.9, 32.6 | 3.988, 52.9, 32.45 | 3.985, 55.4, 32.28 | 3.996, 53.6, 32.7 | 3.987, 53.7,32.50 | 4.007, 53.7,32.98 | 4.016, 54.1, 33.23 | 4.010 54.9,33.08 |
| *r*, *β*, (Cl−H7) | 2.64, 77.6 | 2.64, 77.6 | 2.64, 77.5 | 2.67, 77.5 | 2.69, 77.4 | 2.71, 77.4 | 2.67, 77.6 | 2.66, 78.0 |
| *r*, *β*, (Cl−H1) | 2.83, 27.2 | 2.83, 27.2 | 2.83, 27.4 | 2.85, 27.9 | 2.87, 28.0 | 2.89, 28.1 | 2.87, 28.4 | 2.87, 28.8 |
| $S(T_d)$ $[Fe_4S_4X_4]^{3-}$, $[Fe_4S_4]^{+}$ | 0.612, 0.045 | 0.547, 0.040 | 0.539, 0.037 | 0.233, 0.014 | 0.178,0.010 | 0.196,0.011 | 0.110,0.010 | 0.018, 0.0002 |
| Y···H−C(1)[d] | 2.64 | 2.64 | 2.64 | 2.67 | 2.69 | 2.71 | 2.67 | 2.66 |
| | 3.590(2) | 3.594(2) | 3.590(3) | 3.616(3) | 3.617(4) | 3.633(3) | 3.596(4) | 3.590 |
| | 161 | 160 | 160 | 160 | 161 | 160 | 161 | 159 |
| Y···H−C(7)[d] | 2.83 | 2.83 | 2.83 | 2.85 | 2.88 | 2.89 | 2.87 | 2.87 |
| | 3.634(2) | 3.629(2) | 3.636(3) | 3.657 | 3.655(4) | 3.671(3) | 3.638(4) | 3.655 |
| | 139 | 139 | 139 | 139 | 138 | 139 | 137 | 138 |
| X···H−C(3)[d] | 2.77 | 2.77 | 2.78 | 2.99 | 2.83 | 2.84 | 2.85 | 2.87 |
| | 3.710(2) | 3.702(2) | 3.718(3) | 3.754(4) | 3.753 | 3.764(4) | 3.760(4) | 3.798 |
| | 158 | 158 | 158 | 158 | 158 | 159 | 157 | 158 |
| S*···H−$CH_2$−$CH_2N^+R_3$[d] | 2.80 | 2.80 | 2.82 | 2.86 | 2.87 | 2.90 | 2.88 | 2.90 |
| | 3.766(2) | 3.768(2) | 3.788(4) | 3.830(4) | 3.821 | 3.848(3) | 3.833(4) | 3.86 |
| | 170 | 170 | 170 | 170 | 170 | 170 | 172 | 172 |
| S*···H−C− $N^+R_3$[d] | 2.85 | 2.84 | 2.85 | 2.91 | 2.91 | 2.93 | 2.88 | 2.90 |
| | 3.600(2) | 3.594(2) | 3.604(3) | 3.669 | 3.665 | 3.676 | 3.614(4) | 3.648 |
| | 133 | 133 | 134 | 134 | 135 | 135 | 134 | 144 |
| Cg···$N_{sh}$ | 6.415 | 6.404, | 6.416, | 6.464 | 6.448, | 6.477, | 6.458, | 6.485, |
| Cg···$N_l$ | 6.57 | 6.561 | 6.579 | 6.62 | 6.612 | 6.645 | 6.589 | 6.609 |

[a] Bonds parallel and perpendicular to $S_4$ axis. [b] Compression = distance (perpendicular to − parallel to)/perpendicular distance × 100. [c] Shape parameters: *r* (Å), *β* (°), and Vol (Å$^3$), see refs 4, 37, and CrystalMaker ver. 8.1.4. [d] Hydrogen bond parameters to acceptor A; A···H (Å), A···C (Å), A−H−C (°).

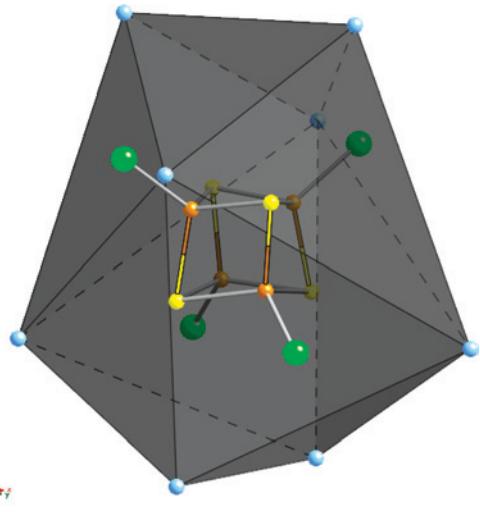

**Figure 3.** The eight cation nitrogen atoms (blue) around the $[Fe_4S_4X_4]^{3-}$ clusters form the vertices of a dodecahedron of elongated (top and bottom pairs of N) and compressed tetrahedra (central four N). The crystallographically imposed $S_4$ axis is vertical, and the longer Fe−S bonds are represented in color.

(PDB:1CKU) surrounded by nine C−H···$\mu_3$-S hydrogen bridges (C···S, 3.517−3.755 Å) and six weaker C−H···S(Cys)−Fe hydrogen bridges (C···S, 3.715−3.840 Å). The concerted nature of a small number of identical supramolecular synthons in small molecule crystals as compared to the large number of very dissimilar interactions in proteins means that the roles of C−H···S interactions are very different in the two environments, even though they are of comparable dimensions.

## Summary

A simple, one-pot synthesis of $(Et_4N)_4[Fe_4S_4Cl_4]Cl$ from iron(II) chlorides and $HS^-$ in aprotic solvents is presented. The subtle effects of C−H···S and C−H···X interactions are more discernible in these simple high-symmetry structures than in those with thiolate ligands. Distortions of the [4Fe−4S] cores from $T_d$ symmetry, as determined using the CSM method, are correlated with the interionic CAHB synthons in the crystal structures. The temperature dependence of these interactions are used to classify those that show only a slight variation in D···A distances as "hard," whereas those with a more substantial temperature dependence are termed "soft." When synthetic models are stripped of their organic groups and the remaining interactions are analyzed in terms of CAHB, it is apparent that the $[4Fe-4S]^+$ cores are inherently of high symmetry and that distortions are the result of their environment. The cocrystallization of a tri-anionic cluster with a chloride results in a symmetric distribution of cations about the anions that is reflected in a more highly symmetric cluster structure than generally occurs with three cations per tetranuclear cluster. Less-symmetric [4Fe−4S] cores have correspondingly less-symmetric distributions of cations around them. Comparable weak hydrogen bridge bonds to those observed here are found in high-resolution protein structures containing $[4Fe-4S]^{2+}$ clusters.

**Acknowledgment.** This research was supported by the University Research Committee at Emory and the Chemistry Department of Emory University. The X-ray Crystallography Center at Emory was made possible in part from funds from the NSF (No. CHE-9974864 single crystal and No. CHE-0541752 powder), and NIH (S10 RR07323 and S10-RR13673). We would particularly like to acknowledge Dr. Kimberly Sessions Hagen of the Center for AIDS Research at Emory for her help in preparing this manuscript.

**Supporting Information Available:** The X-ray tables of crystal data and crystallographic information file (CIF) format, the compilation of CSM data for referenced structures, and the ESI-MS of **1**. This material is available free of charge via the Internet at http://pubs.acs.org.

IC801533Q